World Academy of Science, Engineering and Technology
International Journal of Biomedical and Biological Engineering
Vol:6, No:8, 2012

Effect of Secondary Curvature on Mixing Characteristics within Constant Circular Tubes

Minh Tuan Nguyen , Sang-Wook Lee

***Abstract*—** In this study, numerical simulations on laminar flow in sinusoidal wavy shaped tubes were conducted for mean Reynolds number of 250, which is in the range of physiological flow-rate and investigated flow structures, pressure distribution and particle trajectories both in steady and periodic inflow conditions. For extensive comparisons, various wave lengths and amplitudes of sine function for geometry of tube models were employed. The results showed that small amplitude secondary curvature has significant influence on the nature of flow patterns and particle mixing mechanism. This implies that characterizing accurate geometry is essential in accurate predicting of in vivo hemodynamics and may motivate further study on any possibility of reflection of secondary flow on vascular remodeling and pathophysiology.

***Keywords*—**Secondary curvature, Sinusoidal wavy tubes, Mixing Characteristics, Pulsatile flow, Hemodynamics.

I. Introduction

THERE has been much evidence suggesting that the development of cardiovascular diseases such as atherosclerosis and aneurysm are influenced by local hemodynamic environment. In particular, the wall shear stress, which is known to be one of the most important hemodynamic factors, has been demonstrated to be strongly correlated with biological responses.

In the majority of vascular structure, vessel of interest appears relatively straight, the wall shear stress were estimated based on an assumption of fully developed axisymmetric velocity profile. However, sinusoidal wavy shaped vessels rather than straight tubes can normally be observed in in vivo vascular system. Ford et al. [1] presented that the secondary curvature (minor wiggle) in common carotid artery is not exception, but more common by characterizing the shape and degree of skewing of velocity profile from cine phase contrast magnetic resonance images. Myers [2] also demonstrated the presence and significance of small amplitude out-of-plane curvature in human right coronary artery. This small amplitude sinusoidal wavy geometry may have some clinical implication on the thrombosis and atherosclerosis by the mechanism of secondary flow mixing. In-plane mixing features in helical tubes were investigated [3] and demonstrated that the discrepancy between flow field and the particle trajectories would be explained by considering a combination of translational and rotational reference frame.

Minh Tuan Nguyen is with the Department of Mechanical and Automotive Engineering, University of Ulsan, Ulsan, 680-749 Korea (e-mail: minhtuan710@gmail.com).

Sang-Wook Lee is with the School of Mechanical Engineering, University of Ulsan, Korea (phone: 82-52-259-2765; fax: 82-52-259-1680; e-mail: leesw@ulsan.ac.kr).

In the present study, in order to better understand flow structures and hemodynamic features in sinusoidal wavy-shaped tube models, CFD simulations were conducted with constant pitch of six tube diameters 6D and various curvatures by relatively small amplitudes in steady, periodic and pulsatile inflow conditions based on a representative waveform of carotid flow.

II. Methods

A. Geometry and inflow condition

Sinusoidal curve formulation for the centerline of tube geometry in three dimensional space of Cartesian coordinate can be described as in

$$x = 0$$
$$y = R\,sin(z/c) \quad (1)$$

where the wave length or pitch of the curve is $\lambda = 2\pi c = 6D$ and R is the amplitude of the sine curve. Various amplitudes were considered from $0.1D$ to $0.5D$ with interval of $0.05D$.

A Reynolds number of 250 based on mean flow-rate Q_m and tube diameter, which is in the range of physiological condition, was employed for the steady flow study. For unsteady simulations, two different types flow-rate waveform normalized by mean flow-rate at inlet were imposed at inlet of the tube to investigate the response of inflow as shown in Fig. 1. First one is sinusoidal flow-rate waveform with the same mean value as the steady case, in another word, the same value of Reynolds number with steady simulation was used in this case. The second one is canonical flow-rate waveform that was derived from in vivo measurement in common carotid. In case of this pulsatile flow, Reynolds number of 350 that matches representative physiological conditions in common carotid arteries [4] was used instead of 250 as in the other cases. For all cases, fully developed velocity derived from Womersley flow in rigid pipe was imposed as inflow velocity profile.

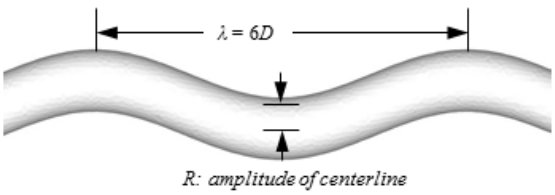

Fig. 1 Geometry of sinusoidal wavy tube

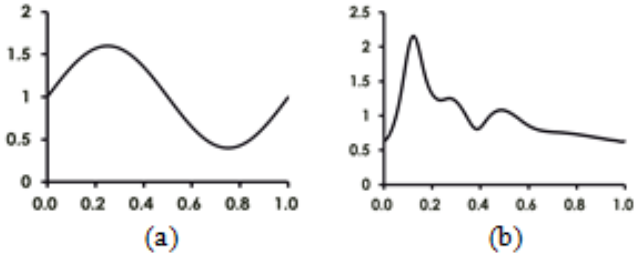

Fig. 2 Inflow flow-rate boundary conditions (a) Sinusoidal flow-rate waveform, (b) Canonical flow-rate wave form

B. Numerical methods

Three-dimensional unsteady incompressible momentum and continuity equations for Newtonian fluid flow were solved as

$$\rho \frac{\partial \mathbf{u}}{\partial t} + \rho \mathbf{u} \cdot \nabla \mathbf{u} = -\nabla p + \nabla \cdot \mathbf{T} \qquad (2)$$
$$\nabla \cdot \mathbf{u} = 0$$

Numerical simulations were carried out by employing a well-validated, in-house CFD solver [5,6] applying quadratic tetrahedral elements based finite element method. Mesh dependence tests were firstly conducted and demonstrated that approximately 300,000 elements was sufficient to ensure mesh independence solutions.

All simulations were run for sufficient time period (or cardiac cycles for unsteady cases) to ensure fully developed flow and damp out the initial transients.

III. Results and Discussion

A. Steady analysis

Axial velocity for three different degree of curvature was extracted at $\mathrm{x} = 25.5\mathrm{D}$ in Cartesian coordinate frame as in Fig. 2(a)-2(c). In overall view, when curvature degree is mild in case of $\mathrm{R} = 0.1\mathrm{D}$, axial velocity profile is similar to the one of Poiseuille flow. However, as the sinusoidal amplitude increases or the curvature increases, peak of axial velocity tends to move downward closer to the tube wall and forms the characteristic crescent shape stream wise velocity profile that can be commonly observed in typical Dean flow inside a curve pipe.

Fig. 2(d)-2(f) show the corresponding axial vorticity contours. Behavior of vorticity in considering cross sections is a combination of symmetric positive and negative vorticity with minor counter-rotating vorticities. The strength of the vorticity becomes stronger as increasing curvature of the tube. Looking at the pattern more deeply, except two strong vorticities that dominant the vorticity field, there are two small vorticities in the core and two weak vorticities nearest the wall. The development and decay of these kinds of vorticity will affect strongly on behavior of velocity field, especially the behavior of flow in a specific section and consequently influence in flow mixing. In steady analysis, since neglecting the effect of time varying, periodic vorticity pattern at considering slice cannot be observed. However, this problem will be dealt with in later part of this study when including sinusoidal or canonical waveform flow-rate at inlet of conduit.

The planar cross-section velocity magnitude profiles overlaid by streamtraces for the in-plane reference were shown in Fig. 2(g)-2(i). The in-plane velocity can be calculated as

$$V_{inplane} = V_{Cartesian} - V_{Translation}. \qquad (3)$$

where the translation velocity can be achieved by taking the derivative of the geometric equation of sinusoidal wavy centerline. Since particle trajectories correspond to the streamtrace pattern, considerable particle mixing can be imagined by the simple sinusoidal wavy tube with relatively small amplitude.

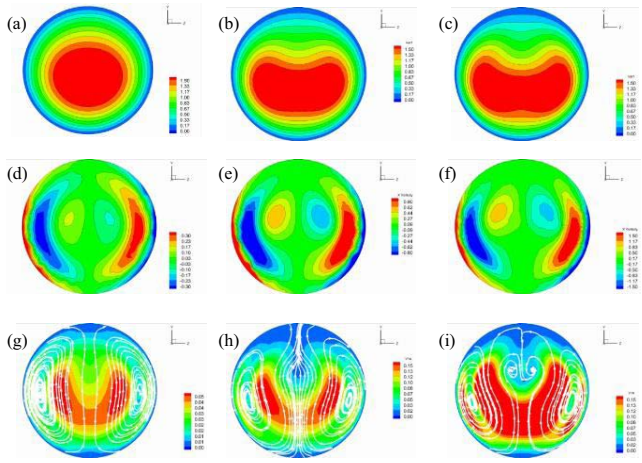

Fig. 3 Axial velocity (the 1st row), axial vorticity (the 2nd row) and in-plane velocity (the 3rd row) contours at x = 25.5D for sinusoidal wavy tube with different amplitude in steady analysis. (a) R = 0.1D, (b) R = 0.3D, (c) R = 0.5D, (d) R = 0.1D, (e) R = 0.3D, (f) R = 0.5D, (g) R = 0.1D, (h) R = 0.3D, (i) R = 0.5D

B. Unsteady analysis – Sinusoidal flow-rate waveform

In Fig. 4, axial velocity, axial vorticity and in-plane velocity for the case $\mathrm{R} = 0.1\mathrm{D}$ were also calculated at the same axial position $\mathrm{x} = 25.5\mathrm{D}$ at four different time points of a cardiac cycle in the same manner as the steady case. Overall flow patterns are similar as those of corresponding steady cases. On the other hand, it can be recognized the presence of unusual axial velocity pattern at the middle of decelerating flow phase, which showing high velocity zone stretched laterally. This type of velocity profile was reported in [7] from magnetic resonance flow measurement in common carotid artery. Although the flow-rate is same at the time points of $t = 0.5s$ and $t = 1.0s$, which are the middle of decelerating and accelerating phase respectively, it was found that different velocity profiles are produced. The influence of modest secondary curvature also generates non-uniform distribution of hemodynamics parameters such as wall shear stress, oscillating shear index and particle residence time which was suggested linked to vascular biology.

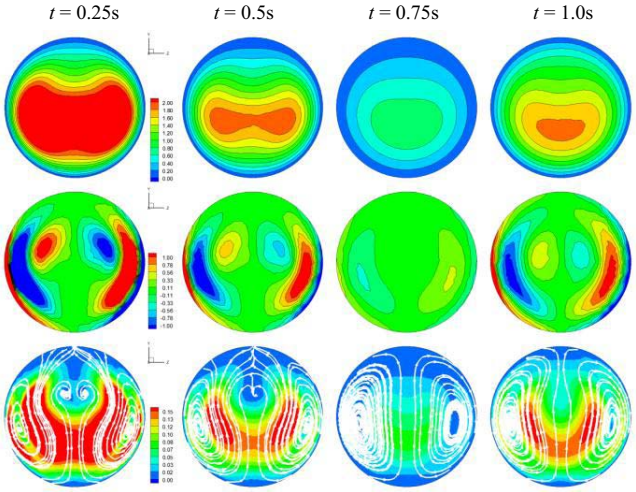

Fig. 4 Axial velocity (the 1st row), axial vorticity (the 2nd row) and in-plane velocity (the 3rd row) contours at x = 25.5D at the different time points (phases) for sinusoidal inflow condition.

C. Unsteady analysis – Pulsatile flow-rate waveform

In this part, the flow is driven by a non-dimensional canonical pulsatile flow as shown in Fig.1 which has been normalized by the value of mean flow-rate at the inlet. The results of axial velocity distribution are shown in Fig. 5. Axial velocity distribution were obtained in several sections A-A, B-B, C-C at locations corresponding to x = 22.5D, x = 24D, x = 25.5D and at different time point in cardiac cycle: peak of systolic t_1 when flow-rate reaches its maximum value, deceleration phase t_2 when flow-rate decrease in magnitude and finally the at time point t_3 peak of diastolic when flow-rate gets its minimum value.

As expecting, when curvature of sinusoidal tube is small, in case of curvature radius equals 0.1D, axial velocity profile resembles a temporal flow in straight pipe. However, as curvature of the pipe increases, as in case of curvature radius equals 0.35D or 0.5D, velocity profile rapidly change to crescent shape which is typical velocity profile shape in curve pipe. At peak of systolic and diastolic phase, symmetrical velocity with axial velocity peak tending to skew upward or downward the wall side according to slice position is evidently shown in case of high curvature tube R = 0.35D and R = 0.5D. In the other hand, under the effect of varying time flow-rate, flow field in high curvature pipe in deceleration phase becomes unstable, the flow seem to separate from the wall, hence result in a asymmetric axial velocity profile.

A similar reaction of axial vorticity distribution was obtained in case of smallest curvature R = 0.1D, flow in this case act like a flow in straight pipe cause of relatively small in curvature. Obviously, at peak systolic, magnitude of vorticity is more considerable when comparing with the other time points in cardiac cycle. When time varies from systolic to diastolic, all available vortex pairs in slice becomes weaker. In case of R = 0.1D, at an interest section, two vortex in the core becomes weaken with time and only a very weak vortex pair remnant at diastolic. Similar behavior was obtained with two stronger vortexes near the wall. Magnitude of this vortex pair decreases as time changes but still dominant at diastolic. Vorticity profile at section A-A and C-C located at middle of the bends is symmetrical similar.

Investigating the vorticity change along the longitudinal direction shows that the growth of axial vorticity pair in the core is weakened by the developing of two contrariwise vorticity near the wall. The two vorticities in the core becomes weaker in next section B-B and nearly dissipates in section C-C. The vorticity pair generated near the wall rolls up, detaches from the wall and becomes stronger and forms a new dominant vorticity in cross section. For preventing this new detached vorticity, nearest the wall, a new pair vorticity is generated and has the same sign with the primary vorticity pair in the core.

In deceleration phase, an unstable occurrence in flow field might cause rotation in vorticity pattern as shown in Fig. 6 in row 2nd of high curvature case R = 0.35D and R =0.5D. In this stage, the primary vorticity in core rotates and can be subsumed by the vorticity near the wall whereas the vorticity near the wall can absorb the same sign single vorticity core or is separated to

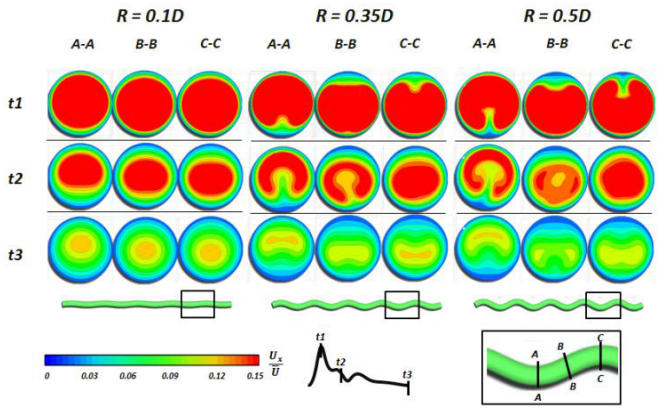

Fig. 5 Axial velocity contour for several curvature tubes: R = 0.1D, R = 0.35D, R= 0.5D at several cross sections A-A, B-B, C-C, at peak of systolic, deceleration and diastolic phase

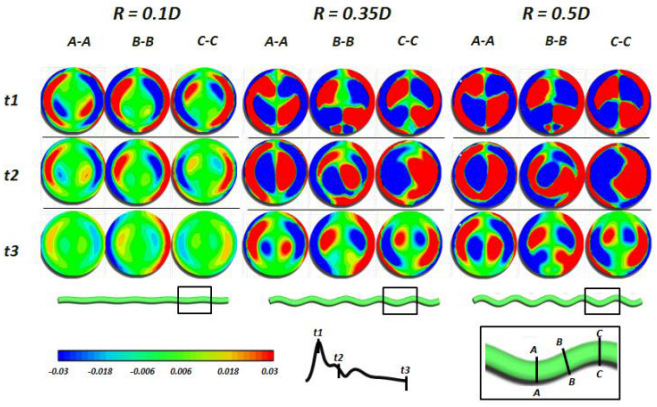

Fig. 6 Axial vorticity contour for several curvature tubes: R = 0.1D, R = 0.35D, R= 0.5D at several cross sections A-A, B-B, C-C, at peak of systolic, deceleration and diastolic phase

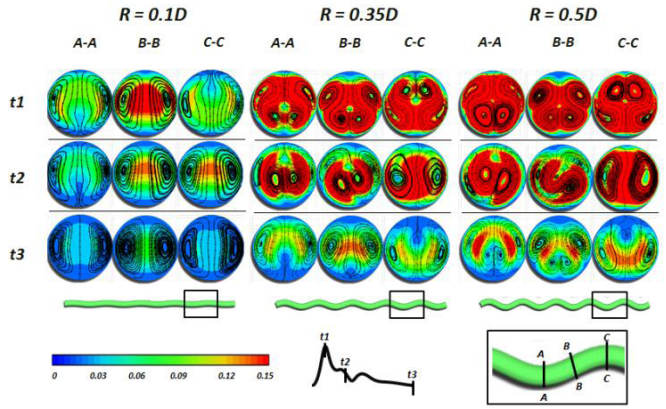

Fig. 7 In-plane velocity contour with streamtrace for several curvature tubes: R = 0.1D, R = 0.35D, R= 0.5D at several cross sections A-A, B-B, C-C, at peak of systolic, deceleration and diastolic phase

form a new small vorticity. This process was represented clearly in Fig 6 at section B-B of R = 0.5D in deceleration phase. Referring to the dominant vorticity distribution in plane of high curvature tube, division vorticity pattern into four parts by order of vorticities indicates that there are four main dominant vortexes occurring in cross section. In case of less curve pipe R = 0.1D, there are only main two vortexes observed in cross section even at time of systolic when velocity is relatively high.

The planar cross section velocity magnitude profiles overlaid by streamtraces pattern for pulsatile flow were shown in Fig.7. The results were obtained in the same manner with the one in steady case and at the same position and three different time point as the previous work for axial velocity and axial velocity distribution. In-plane velocity and streamtraces results revealed the behavior of fluid particles in a plane after subtracting translation motion. As only recording merely the motion of fluid in a plane, in-plane velocity closely relate to the in-plane mixing or stirring that was proposed to influence on preventing activated platelets from residing near the wall and severely accumulating [3]. Velocity in-plane in Fig. 7 also shows that increasing tube curvature leads to a higher velocity field

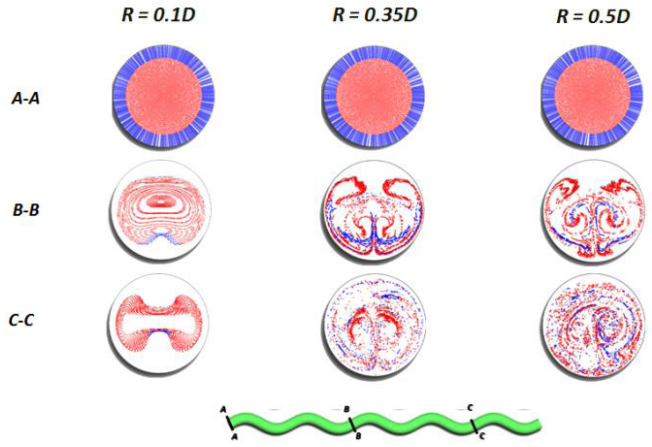

Fig. 8 Particle trajectory slices taken in deceleration phase for several curvature tubes: R = 0.1D, R = 0.35D, R= 0.5D at several cross sections A-A, B-B, C-C

in-plane, and there are four vortexes occur with stronger intensity dominant section instead of only two vortex in case of R = 0.1D. Rotation in flow one more time was obtained by the effect of pulsatile flow at deceleration phase when curvature of tube is relative high.

Mixing behavior at several sections in Fig. 8 was obtain by tracking the motion of mass-less particle through velocity field.

Position of particles beginning from initial slice at inlet, section A-A, were achieved by numerically integrating the advection equation, shown in (4). The 4th order Runge-Kutta integration scheme was used to get the solutions.

$$\frac{dx}{dt} = u(x,t) \tag{4}$$

As expecting, mostly no mixing occurred even in location far downstream far from inlet in case of small curvature R = 0.1D. In a contradictory manner, more curve tube enhanced in-plane mixing. Particles near the wall moved inside the core, whereas fluid particle in core in turn roll up to outside wall and so on along the length of tube. Consequently, strong mixture results were captured in case of R = 0.35D and R =0.5D at section C-C far from the inlet.

IV. Conclusion

Although the amplitude of secondary curvature of constant radius pipe is relatively small, it was revealed that it creates significant influence on the nature of flow patterns and particle mixing mechanism. This implies that characterizing accurate geometry is essential in accurate predicting of in vivo hemodynamics and may motivate further study on any possibility of reflection of secondary flow on vascular remodeling and pathophysiology.

Acknowledgment

This work was supported by National Research Foundation grant funded by the Korea government (2010-0025683).

References

[1] M. Ford, Y. Xie, B. Wasserman, and D. Steinman, “Is flow in the common carotid artery fully developed?” Physiol. Meas., Vol. 29, 2008, pp. 1335-1349.
[2] J. Myers, J. Moore, M. Ojha, K. Johnston, and C. Ethier, “Factors influencing blood flow patterns in the human right coronary artery,” Ann. Biomed. Eng., Vol. 29, 2001, pp. 109-120.
[3] A.N. Cookson, D.J. Doorly, and S. J. Sherwin, “Mixing through stirring of steady flow in small amplitude helical tubes,” Ann. Biomed. Eng., Vol. 37, 2009, pp. 710-721.
[4] S.-W. Lee, L. Antiga, J.D. Spence, D.A. Steinman, Geometry of the carotid bifurcation predicts its exposure to disturbed flow,” Stroke, Vol. 39, 2008, pp. 2341-2347.
[5] C. Ethier, S. Prakash, D. Steinman, R. Leask, G. Couch, and M. Ojha, “Steady flow separation pat-terns in a 45 degree junction,” Journal of Fluid Mechanics 411, 2000, 1–38.
[6] C. Ethier, D. Steinman, and M. Ojha, “Comparisons between computational hemodynamics, photochromic dye flow visualization and magnetic resonance velocimetry. In: Xu, X.Y., Collins, M.W.E. (Eds.), The hemodynamics of arterial organs: comparison of computational predictions with in vivo and in vitro data,” WIT Press, 1999, pp. 131–183.
[7] A. Wake, “Modeling fluid mechanics in individual human carotid arteries,” PhD thesis, Georgia Institute of Technology, 2005.